Thin Solid Films 519 (2010) 31–36

Contents lists available at ScienceDirect

Thin Solid Films

journal homepage: www.elsevier.com/locate/tsf

Room temperature deposition of Al-doped ZnO films on quartz substrates by radio-frequency magnetron sputtering and effects of thermal annealing

Weifeng Yang [a], Zhengyun Wu [a,*], Zhuguang Liu [a], Aisuo Pang [a], Yu-Li Tu [b], Zhe Chuan Feng [b,*]

[a] Department of Physics, Xiamen University, Xiamen 361005, PR China
[b] Department of Electrical Engineering, National Taiwan University, Taipei 106-17, Taiwan

ARTICLE INFO

Article history:
Received 23 May 2009
Received in revised form 1 July 2010
Accepted 9 July 2010
Available online 16 July 2010

Keywords:
Aluminum oxide
Hall effect
Optical properties
Quartz
Sputtering
X-ray diffraction
X-ray photoelectron spectroscopy (XPS)
Zinc oxide

ABSTRACT

High-quality Al-doped zinc oxide (AZO) thin films have been deposited on quartz substrates by radio-frequency magnetron sputtering at room temperature for thin film solar cell applications as transparent conductive oxide (TCO) electrode layers. Effects of post-deposition annealing treatment in pure nitrogen and nitrogen/hydrogen atmosphere have been investigated. Annealing treatments were carried out from 300 °C to 600 °C for compatibility with typical optoelectronic device fabrication processes. A series of characterization techniques, including X-ray diffraction, scanning electron microscopy, Hall, optical transmission, and X-ray photoelectron spectroscopy has been employed to study these AZO materials. It was found that there were significant changes in crystallinity of the films, resistivity increased from 4.60×10^{-4} to 4.66×10^{-3} Ω cm and carrier concentration decreased from 8.68×10^{20} to 2.77×10^{20} cm^{-3} when annealing in 400 °C pure nitrogen. Whereas there were no significant changes in electrical and optical properties of the AZO films when annealing in 300–500 °C nitrogen/hydrogen atmosphere, the electrical stability of the AZO films during the hydrogen treatment is attributed to both desorption of adsorbed oxygen from the grain boundaries and production of additional oxygen vacancies that act as donor centers in the films by removal of oxygen from the ZnO matrix. These results demonstrated that the AZO films are stably suited for TCO electrodes in display devices and solar cells.

1. Introduction

Heavily doped ZnO films have recently been recognized as a potential replacement transparent conductive oxide to the industry standard tin-doped indium oxide (ITO). They are transparent at visible wavelength ranges, have direct and wide band gap (E_g>3.30 eV at room temperature), and have a large exciton binding energy (~60 meV at room temperature). Such properties make ZnO well suited for the realization of many optoelectronic applications including transparent conductive oxides in display devices and solar cells [1–4]. Recent researches demonstrated that B, Al, Ga, In, and F doped ZnO films reveal both low resistivity and high transmittance in the visible region [5–8]. Among these, Al-doped ZnO (AZO) has similar electrical and optical properties to ITO, but comparing to which, AZO possesses advantages of a nontoxic material, with high temperature stability, and costs less to manufacture [9].

Different technologies such as electron beam evaporation [10], sol–gel [11], chemical spray [12], pulsed laser deposition [13], direct-current and radio-frequency (RF) magnetron sputtering [14], etc. have been reported to produce thin films of AZO with adequate performance for applications. However, these deposition techniques, while yielding high-quality films, require relatively high temperatures [14,15], which are incompatible with plastic substrates or sensitive photoresist as those used in light emitting diodes and solar cells, especially in lift-off fabrication technology. Moreover, there are some reports [16–20] on annealing of the AZO films deposited at high temperature substrate, but yet there are very few reports on annealing of the AZO films deposited at room temperature (RT). In this paper, high performance AZO thin films were grown by RF magnetron sputtering RT, and a systematic study of annealing effects on the structural, electrical, and optical properties of the AZO thin films in different temperatures and different atmospheres has been discussed in detail.

2. Experimental details

The AZO films were deposited on quartz substrates in a SP-2 RF magnetron sputtering system with a base pressure of 4×10^{-4} Pa and at RT. A sintered ceramic sputter target with a mixture of ZnO (99.99% purity) and Al_2O_3 (99.99% purity) was employed as source material. The content of Al_2O_3 added to the sputter target was 2% in weight. The sputtering power, Ar flow rate, and the distance between sputter target and substrate were optimized at 300 W, 30 sccm, and 7 cm, respectively. Details of the AZO deposition process have been reported elsewhere [21]. The as-deposited AZO films were subsequently conventionally heat-treated for 15 min in pure N_2 and N_2 with 4% hydrogen atmosphere by varying the annealing temperature from

* Corresponding authors. Tel.: +886 2 3366 3543; fax: +886 2 2367 7467.
E-mail addresses: zhywu@xmu.edu.cn (Z. Wu), fengzc@cc.ee.ntu.edu.tw (Z.C. Feng).

0040-6090/$ – see front matter © 2010 Elsevier B.V. All rights reserved.
doi:10.1016/j.tsf.2010.07.048

300 °C to 600 °C. This temperature was chosen since it is known as the maximum range in typical device processing.

A series of analytical technologies was employed to characterize and investigate the polycrystalline AZO materials. The structural properties of the AZO films were analyzed with a Panalytical X'pert PRO powder X-ray diffractometer which uses a Cu-Kα radiation (λ = 0.15406 nm). The surface morphology and section shape of the AZO films were examined by using a field emission scanning electron microscopy (SEM) LEO 1530. The optical transmission spectra of the AZO films were measured from a Cary 5000 spectrophotometer. The film thickness was determined through a Dektak3 surface profile measurement system. The resistivity, carrier concentration and carrier mobility of the AZO films were acquired by way of an Accent HL5500 Hall System with a four-point probe. The chemical state in the films was investigated by means of X-ray photoelectron spectroscopy (XPS) using a PHI Quantum 2000 Scanning ESCA Microprobe instrument.

3. Results and discussion

3.1. Structural features studied via X-ray diffraction

Fig. 1 shows X-ray diffraction (XRD) patterns for the AZO thin films, as-grown and annealed from 300 °C to 600 °C in N_2 and $N_2 + 4\%$ H_2 atmosphere, respectively. All of the AZO thin films gave strong (002) diffraction peaks. Other peaks (004) with much less intensity were observed, with no obvious metallic zinc, aluminum, or ZnAlO characteristic peaks found. These indicate that all the experimental AZO films grown on quartz substrates exhibit a strong c-axis orientation perpendicular to the substrate surface.

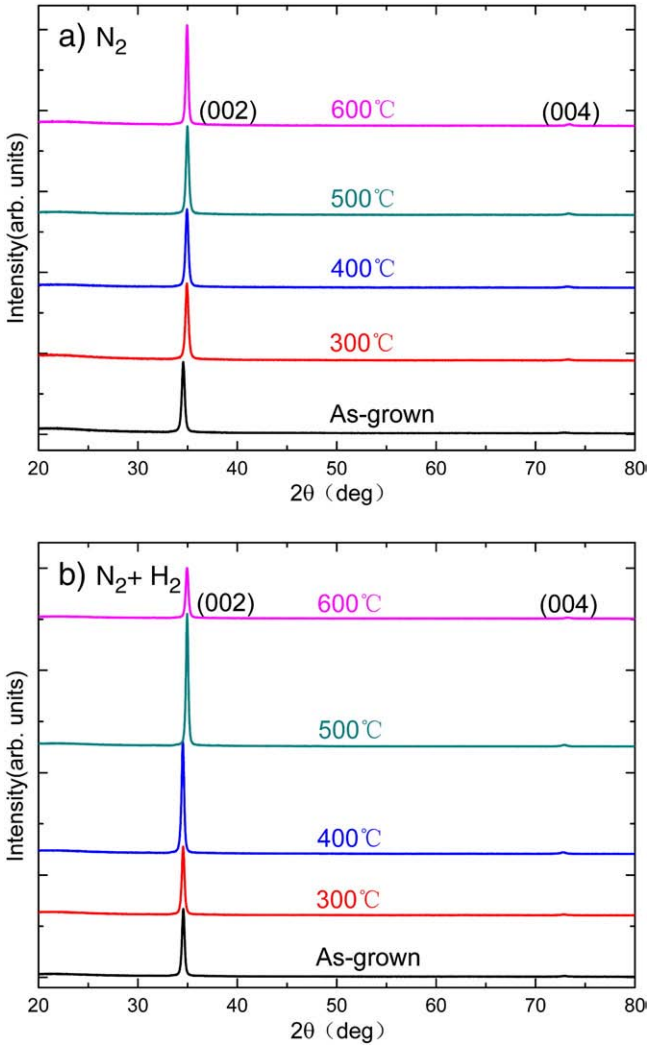

Fig. 1. XRD patterns of the as-grown and post-annealed AZO films at 300 °C–600 °C for 15 min in (a) N_2, and (b) $N_2 + 4\%$ H_2.

To compare the structure features of the AZO films, the full-width at half-maximum (FWHM) of the XRD (002) peak and the crystallite dimension are listed in Table 1. The FWHM values for AZO/quartz were found to decrease from 0.271 to 0.262° as annealed in N_2 from 300 °C to 600 °C and decreased to 0.265° for annealed in $N_2 + H_2$ from 300 °C to 500 °C, while increased to 0.283° at 600 °C.

The grain size of the films can be calculated according to Scherrer relation [20]:

$$D = (0.9\lambda) / \beta \cos\theta \quad (1)$$

where λ is the X-ray wavelength, 0.154 nm, and β = B − b where B is the observed FWHM and b is the instrument function parameter determined from the broadening of the monocrystalline silicon diffraction peak. The obtained grain size (D) values for the experimental AZO films are listed in Table 1, being in range of 30.5–35.2 nm. For the samples annealed in N_2, D increased slightly from as-grown one to annealing till 400 °C, and reached a highest value of 35.2 nm for annealing at 600 °C. For annealing in $N_2 + H_2$, D also increased from as-grown one to annealing till 500 °C, reached a highest value of 34.8 nm for annealing at 500 °C, but decreased to a low value of 30.5 nm at 600 °C. The grain size values have showed similar trend with the annealing conditions as XRD FWHM does.

The improvement in crystallinity by annealing may be explained by the increase in grain size and the decrease of point defects such as oxygen vacancy and zinc interstitial as the annealing temperature increases. While the weakening in crystallinity by annealing at 600 °C in $N_2 + H_2$ could be due to the decrease of grain size and destruction of film surface perfection which were resulted from oxygen species on surface combined by hydrogen contamination atoms.

3.2. Surface morphology and status

The surface morphologies of the as-grown and post-annealed AZO thin films were examined by SEM and are shown in Fig. 2. The films are composed of closely packed nanocrystallites. The grain size of the as-grown AZO film is directly seen to increase with increasing annealing temperature in N_2 as revealed from XRD data analysis in the last section. Different morphologies were observed for the AZO films grown on quartz with increasing annealing temperature. Fig. 2b) shows the cross-sectional SEM micrograph of the as-grown sample. The film grows in a columnar structure vertical to the substrate, being consistent with the XRD measurement results (c-axis orientation). However, the upper section of the fracture edge does not show this clear structure, which was possibly caused by the destruction during the cutting process. Porous surface was found on the AZO thin films when annealing at 600 °C in $N_2 + 4\%$ H_2, as shown in Fig. 2f), which

Table 1
The structural properties and atomic percent for the AZO films as-deposited and annealed in different atmospheres.

Sample	002 peak (°)	FWHM (°)	Grain size (nm)	O (at.%)	Zn (at.%)	Al (at.%)
As-deposited	34.55	0.271	33.0	47	50	3
N_2, 400 °C	34.94	0.271	33.1	42	55	3
$N_2 + H_2$, 400 °C	34.57	0.270	33.3	48	49	3
N_2, 600 °C	34.96	0.262	35.2	41	56	3
$N_2 + H_2$, 600 °C	34.94	0.283	30.5	45	53	3